https://ntrs.nasa.gov/search.jsp?R=19790009726 2020-03-22T01:18:58+00:00Z

General Disclaimer

One or more of the Following Statements may affect this Document

- This document has been reproduced from the best copy furnished by the organizational source. It is being released in the interest of making available as much information as possible.

- This document may contain data, which exceeds the sheet parameters. It was furnished in this condition by the organizational source and is the best copy available.

- This document may contain tone-on-tone or color graphs, charts and/or pictures, which have been reproduced in black and white.

- This document is paginated as submitted by the original source.

- Portions of this document are not fully legible due to the historical nature of some of the material. However, it is the best reproduction available from the original submission.

Produced by the NASA Center for Aerospace Information (CASI)

NASA

Technical Memorandum **79719**

Changes in the Terrestrial Atmosphere-Ionosphere-Magnetosphere System Due to Ion Propulsion for Solar Power Satellite Placement

S. A. Curtis and J. M. Grebowsky

FEBRUARY 1979

National Aeronautics and
Space Administration

Goddard Space Flight Center
Greenbelt, Maryland 20771

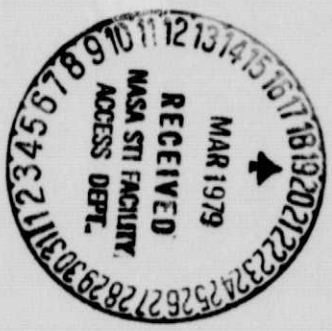

CHANGES IN THE TERRESTRIAL ATMOSPHERE-IONOSPHERE-MAGNETOSPHERE SYSTEM DUE TO ION PROPULSION FOR SOLAR POWER SATELLITE PLACEMENT

S. A. Curtis and J. M. Grebowsky

NASA/Goddard Space Flight Center
Laboratory for Planetary Atmospheres
Greenbelt, Maryland 20771

ABSTRACT

We give preliminary estimates of the effects massive Ar^+ injections have on the ionosphere-plasmasphere system with specific emphasis on potential communications disruptions. The effects stem from direct Ar^+ precipitation into the atmosphere and from Ar^+ beam induced precipitation of MeV radiation belt protons. These injections result from the construction of Solar Power Satellites using earth-based materials in which sections of a satellite must be lifted from low earth to geosynchronous orbit. The most plausible method of accomplishing this task is by means of ion propulsion based on the relatively abundant terrestrial atmospheric component, Ar. The proposed propulsion system will release a dense beam of $\sim$5 keV Ar^+ (Hanely and Guttman, 1978a). The total amount of Ar^+ injected in transporting the components for each Solar Power Satellite is comparable to the total ion content of the ionosphere-plasmasphere system while the total energy injected is larger than that of this system. It is suggested that such effects may be largely eliminated by using lunar-based rather than earth-based satellite construction materials.

INTRODUCTION

We wish to examine the possible environmental impacts of one aspect of Solar Power Satellite (SPS) construction involving the lifting of SPS components from low earth orbit (LEO) to geosynchronous earth orbit (GEO) using ion propulsion spacecraft powered by solar arrays. In current studies, this is the second stage of a two step process envisioned when terrestrial materials are used in SPS construction (Hanely and Guttman, 1978a). The first step is lifting materials from the earth's surface to LEO with a heavy lift launch vehicle (HLLV) which is planned to be an enlarged later generation of the current Space Shuttle. In the second step, orbital transfer vehicles (OTV) will inject $\sim 2 \times 10^6$ kg of ~ 5 keV argon ions into the near earth environment in the process of carrying the components that will comprise the $\sim 37.5 \times 10^6$ kg SPS from LEO to GEO. The use of ion propellants is necessitated by the prohibitive demands of chemical propellants. It is this massive release of energetic ions in the upper ionosphere, the plasmasphere and the outer magnetosphere that is the subject of this paper. This is viewed as giving rise to significant man made perturbations of the earth's atmosphere, ionosphere and magnetosphere.

Vehicle and Orbit Description

The basis of our investigation is formed by recent studies of orbital operations for SPS construction (Hanely and Guttman, 1978b). These studies indicate that the SPS components will be carried from LEO to GEO by about 10 OTV's. Each OTV will consist of a solar array of ∿260 1 megawatt ion thrusters having an area of $\sim 10^7 cm^2$. This thruster array will be attached by cables to the partially assembled SPS structure to be moved to GEO as shown in Figure 1. The thrusters' fuel is argon due to its relatively high abundance (∿1% of total atmosphere) and low cost. Additionally, the relatively low first and high second ionization potentials of Ar as well as its high specific impulse and thrust resulting from its intermediate weight also make it a reasonable choice (Stuhlinger, 1964). An OTV will require ∿130 days for the LEO to GEO transfer. Thus, all of the OTV vehicles will be flying almost simultaneously since the desired building rate of SPS is projected at one per ∿180 days. The transport of the SPS materials from earth to LEO is limited to ∿50 days and thus a high launch frequency of the HLLV's is required. The total number of SPS's envisioned to supply a substantial amount of the U.S. electrical power requirements will require construction and transport over a period of decades (Glaser, 1977). The transfer orbit from LEO to GEO will be a spiral that is most tightly wound at lower altitudes. Hence the OTV's will be spending most of their time near the earth where most of the deposition of the 5 keV Ar^+ will occur, tending to maximize environmental effects there. The ion beam emitted by the OTV will have a velocity spread of ∿0.4 V_b where V_b = 150

km sec^{-1} is the beam velocity. The beam will therefore spread rapidly during the time it remains in the plasmasphere (100-200 sec). Typical plasma parameters for an OTV are shown in Table 1.

Ion Beam Dynamics

The 5 keV Ar^+ beam emitted by the ion propulsion thruster array of the OTV's is the source of the environmental effects we wish to discuss here. We will first consider the time evolution of the beam following its injection from a given orbital position near the earth's equatorial plane.

The thrusters' beam is directed approximately perpendicular to the local magnetic field lines. Its propagation characteristics have been discussed by a number of authors (Heikkila, 1978; Schmidt, 1966; Falthammar, 1973). The essential characteristics are that most of the ions travel at a velocity V_b equal to the beam's exit velocity from the ion thrusters until the beam density becomes sufficiently low so that the Ar^+ no longer acts collectively to maintain the polarization electric field needed for cross-field propagation. The critical number density below which the beam density n_b must fall to stop propagation is

$$n_c = \frac{B^2}{4\pi m_A c^2} \qquad (1)$$

where B is the terrestrial magnetic field strength, m_A is the argon ion mass and c is the speed of light. Equation (1) is equivalent to saying that the magnetic field energy density must be greater than the rest mass energy density of the beam and follows directly from the beam propagation equations (Falthammar, 1973). In addition, equation (1) implies that the plasma dielectric constant is near unity. For outward propagating beams the condition $n_b < n_c$ cannot be satisfied within the plasmasphere. In Figure 2 we show the beam densities and critical

densities as functions of time from injection for injection at L=1.5 (note that LEO is at L $\tilde{\sim}$ 1.1). As can be seen from this figure n_c is always much less than n_b and the beam is not stopped in the near-earth plasma environment. Beam-plasma instabilities are ineffective in stopping the beam. The instability growth periods are characteristically on the order of $\tau_g \sim \frac{n_p}{n_b} \tau_A$ where n_p is the ambient background plasma density and τ_A is the argon ion gyroperiod. Since $n_p \sim 10^3$, we see from Figure 2 that $n_p >> n_b$ due to rapid beam spreading and hence τ_g is not small compared to the beam's residence time in the plasmasphere. Additionally, the low conversion efficiency of beam energy into plasma wave turbulence further reduces the beam stopping power due to instabilities produced during the beam's brief transit through the plasmasphere (Palmadesso et al., 1976).

Since the Ar^+ beam is not stopped in the plasmasphere and the residence time of the beam in the plasmasphere is only ∿200 sec it is worthwhile to ask what effects the beam has on the plasmasphere and upper ionosphere. Although the beam is not stopped and most of the beam escapes the plasmasphere, a substantial fraction of the beam mass is deposited in the plasmasphere. The mechanism for this deposition derives from the fact that the polarization electric field E_p that allows cross field propagation is nonuniform across the beam's cross section (Crow et al. 1978). Specifically, in the outer sheath of the beam the ions are subject to a smaller polarization field and hence will fall behind the bulk of the beam. This may be visualized as a process in which successive onion skin-like layers are peeled off of an expanding beam. The lost

ions are then bound to the field lines since they now lack the electric field required for $\underline{E}\times\underline{B}$ cross-field movement. The characteristic width of this beam sheath will be the Debye length of the beam plasma

$$\lambda_D \approx \left[\frac{m_A(\Delta V_b)^2}{8\pi n_b e^2}\right]^{1/2} \tag{2}$$

where ΔV_b is the beam spread in velocity, $\Delta V_b \sim 0.4\ V_b$. To estimate the fraction of the beam lost per unit time we regard all the ions in the beam's Debye sheath to be lost and the characteristic refilling time of the sheath to be the local Ar^+ gyroperiod

$$\tau_A(L) = \tau_A(L=1.0)\ L^3 \tag{3}$$

where $\tau_A(L=1.0)=0.08$ sec is the Ar^+ gyroperiod at the earth's surface. This model for the loss process, although simplified for computational ease, embodies the basic physics of the beam loss process and should yield results correct in order of magnitude. Now let N be the line density of the beam obtained by integrating the beam's density over its cross section. The fractional loss in a gyroperiod is then

$$f_{loss} = 1 - (1-\lambda_D/a)^2 \approx 2\lambda_D/a \tag{4}$$

where a is the beam's radius and $\lambda_D/a \approx 10^{-4}$. Then the change in the beam line density per unit time is

$$\frac{dN}{dt} = \frac{-2\lambda_D}{a}\ \frac{N}{\tau_A} \tag{5}$$

The beam trajectory is given by

$$L(t) = (L_o^2 + V_b^2 t^2 / R_e^2)^{1/2} \tag{6}$$

where L_o is the beam's injection position and R_e is the radius of the earth. We note that the effects of drifts due to gradients and curvature in the terrestrial magnetic field (assumed dipolar) are negligible. Since $\lambda_D \propto N^{-1/2}$ we obtain upon integration of equation (5)

$$f(t) = 1 - \frac{N(t)}{N_o} \approx \frac{0.124}{L_o^2} \sin \tan^{-1} \frac{V_b t}{L_o R_e} \tag{7}$$

where $f(t)$ is the fractional loss of the beam's line density at time t. N_o is the initial beam line density at injection ($t=0$). We observed from (7) that as $t \to \infty$ the asymtotic value approached for the fractional beam depletion is

$$f(t \to \infty) \approx 0.124\ L_o^{-2} \tag{8}$$

Thus, the greatest local deposition of Ar^+ is achieved by injection at the smaller L values and is $\sim 10\%$. In Figure 3 we plot the fractional beam depletion as a function of radial distance in the earth's equatorial plane for a number of different injection positions. Characteristically the beam will deposit a few percent of its total mass in the plasmasphere before leaving. Not only is greater deposition produced by beam injection closer to earth, as implied in equation (7), but since the OTV's trajectory is a spiral, most tightly wound at lower altitudes, the time for deposition is also greater there. The time spent between the radial position L_1 and L_2 by the OTV is given by

$$t \approx \frac{GMm_{OTV}}{P} \left(\frac{1}{L_1} - \frac{1}{L_2}\right) \left(1 - \frac{\tan^{-1}}{\pi} \frac{1}{(L_{12}^2-1)^{1/2}}\right)^{-1} \qquad (9)$$

where P is the effective power of the OTV ion thrusters G is the gravitational constant M the mass of the earth, m_{OTV} the OTV mass and $L_{12} = \frac{L_1 + L_2}{2}$. In equation (9) we have also accounted for the time spent in the earth's shadow by the OTV. During times of solar eclipse the OTV will not be operating since it is solar powered. Using the trajectory given by equation (9) and the fractional deposition rate given by equation (7), we have computed the total deposition of Ar^+ in the plasmasphere as a function of radial distance from earth. The Ar^+ is assumed to be uniformly distributed between $\pm 30°$ latitudes. The results of this calculation are shown in Figure 4, where we see that the energetic Ar^+ deposited in the plasmasphere will constitute roughly 1-10% of the plasmasphere's natural cold plasma density of $\sim 10^3$ cm^{-3}. This means that the energy density of Ar^+ per SPS will be roughly two orders of magnitude greater than the cold plasma background. It is this artifically introduced plasma component which will produce environmental effects.

Since a substantial number of the ions injected by the OTV's at orbits well within the plasmasphere propagate out beyond the plasmapause into the outer magnetosphere, modifications may be expected there. Typical outer magnetosphere densities are $\sim$ 1 cm^{-3} and temperatures $\sim$ 1 keV, thus, the beam ions will represent a substantial energetic high-Z source. The injection of these high-Z ions into the magnetotail may increase anomalous resistivity and hence the rate of magnetic field

line merging (private communication, C. S. Wu). Due to the possible causal connection between merging and substorms (Hultquist, 1969), the result could be an increased frequency of magnetospheric substorms with potentially disruptive effects on the high latitude ionosphere and radio communications. An increase in auroral activity may also be expected.

Lifetimes of Deposited Argon Ions

There exist three principal loss mechanisms for the Ar^+. These are (1) charge exchange with the exospheric hydrogen, (2) coulomb scattering with plasmasphere electrons and (3) plasma instability-induced pitch angle scattering which results in the precipitation into the atmosphere. In the charge exchange (CE) process the Ar^+ is lost by conversion into a hot neutral Ar atom. The atoms are not bound to the magnetic field lines and depending on their initial velocity are either lost in the atmosphere or escape from the earth. Electron coulomb scattering (ECS) will heat the plasmasphere electrons and slow the energy degradation rate of the Ar^+. The long term result of ECS is the thermal assimilation of energetic Ar^+ into the plasmasphere. Finally, plasma instabilities (PI) driven by the pitch angle anisotropy of the energetic Ar^+ provide a free energy source to generate plasma turbulence which will cause the Ar^+ to randomly walk in pitch angle and hence to partially fill in the loss cone. The initial Ar^+ anisotropy is due to their injection nearly perpendicular to the geomagnetic field. Thus, the contents of the partially filled loss cone will be dumped into the atmosphere at each mirroring point, reducing the fluxes of Ar^+. Also the Ar^+ will tend to assimilate into the plasmasphere background plasma by heating the background plasma in a two stage process in which the Ar^+ first generates plasma turbulence. The turbulence is then damped by the cold plasmasphere plasma which is heated in the process. We consider each of these processes in greater detail.

The charge exchange interaction involves the reaction

$$H(^2S) + Ar^+ (^2P_{3/2}) \rightarrow H^+ + Ar (^1S_o) \qquad (10)$$

where neutral H is the dominant component of the terrestrial exosphere, the collisionless uppermost layer of the atmosphere that gradually merges into the interplanetary medium. We note that the position of LEO is somewhat higher than the nominal position of the base of the exosphere located at ~500 km. Using a model exosphere (Hartle, 1971) for the radial variation of H, we have calculated the lifetime of Ar^+ as a function of radial distance by means of the principle of detailed balance (Mapleton, 1972) and known charge exchange cross sections (Stedeford and Hasted, 1955). The results of this calculation are shown in Figure 5 by the dotted line. Although the lifetime τ_{CE} is only a few days near the exobase at LEO (L=1.1), it rapidly increases with increasing distance and becomes characteristically of the order of months throughout most of the plasmasphere.

Electron coulomb scattering is directly proportional to the electron temperature to the 3/2 power and inversely proportional to the ambient electron density (Spitzer, 1967; Montgomery and Tidman, 1964) in the regime where $v_{the} >> V_b >> v_{thi}$, the relationship between the Ar^+ velocity, the electron thermal velocity v_{the} and the ion thermal velocity v_{thi} in the plasmasphere. Thus the lifetime of Ar^+ determined by ECS will depend sensitively on the extent to which the background plasmasphere electrons are heated. The dominant loss caused by ECS is the energy degradation of Ar^+ due to the small electron to ion mass ratio. The effects of pitch angle scattering caused by the much lighter electrons

or plasmasphere protons are negligible. Now the ability of the energetic Ar^+ to heat the plasmasphere electrons significantly and thus to extend their lifetimes, limited by ECS depends on the relative energy content of the plasmaspheric electrons and the Ar^+. In Figure 4 we see that the ratio of Ar^+ density to electron density is $n_A/n_e \sim 10^{-1} - 10^{-2}$ and since $T_A/T_e \sim 5x10^3$ we find that $n_A T_A/n_e T_e \sim 50\text{-}500$. Thus appreciable heating of the plasmasphere electrons will occur during the energy degradation of the Ar^+. The level of plasmasphere electron heating will be limited by the effects of electron heat conduction transporting this energy out of the plasmasphere and into the ionosphere. In Figure 5 we show by the solid lines the ECS lifetime T_{ECS} for modest plasmasphere electron temperature increases relative to those possible from the energy reservoir represented by energetic Ar^+. We see that until plasmasphere temperatures greater than 10 eV are attained, the ECS loss process dominates the CE loss process except for altitudes below L=2. The density model used in these calculations had densities varying exponentially from 10^4 cm^{-3} at LEO to $\sim 10^3 cm^{-3}$ near the plasmapause. Beyond the plamasphere (since $\tau_{ECS} \propto T_e^{3/2}/n_e$, and the outer magnetospheric plasma is hot and tenuous, i.e., $T_e \sim 1$ keV, $n_e \sim 1$) the CE loss process yields lifetimes orders of magnitude smaller than those of ECS.

The last loss process we consider is that due to the plasma instabilities. The initially anisotropic Ar^+ will drive plasma turbulence by means of the ions' excess free energy until a limiting flux condition is satisfied (Kennel and Petschek, 1966). In this situation any increase in the pitch angle anisotropy of Ar^+ will tend to increase the rate of

scattering of these ions into their loss cones and hence to decrease their flux and anisotropy levels. The rate at which this steady state situation is approached will depend on the growth periods of plasma instabilities driven by the Ar^+ excess free energy, on the rate at which this turbulence scatters Ar^+ into loss cones, on the bounce period of Ar^+ between mirroring points and on the size of the loss cone at a given equatorial radial distance, L. Now the characteristic growth period τ_g is given by (Mikhailovskii, 1974, 1975),

$$\tau_g \sim \frac{n_e}{n_A} \tau_A \qquad (11)$$

where τ_A is the Ar^+ gyroperiod which ranges from 0.1 to 26 seconds from L = 1.1 to L = 6.6 and since $n_A/n_e \sim 10^{-1} - 10^{-2}$ the typical growth periods range from little more than a second at LEO to at most a few minutes within the plasmasphere. Since the saturation turbulence levels due to the instabilities may be expected to occur within several growth periods (Davidson, 1972), we may expect the turbulence to be well established anywhere in the plasmasphere in less than about one hour after beam passage. If we assume that the turbulence level is high enough to isotropize the Ar^+ in p bounce periods τ_b the lifetime of Ar^+ with respect to plasma instabilities is

$$\tau_{PI} \sim \frac{p\tau_b}{2(1-\cos \alpha_o)} \qquad (12)$$

where α_o is the loss cone angle at a given radial distance L. α_o varies from $\sim 60^\circ$ at L=1.1 to only a few degrees at $L \gtrsim 2.0$. The bounce periods vary from $\tau_b \sim 1$ min at L=1.1 to $\tau_b \sim 10$ min at L = 4.0 (Schulz and Lanzerotti,

1974). In deriving equation (12) we assume that in p bounce periods the loss cone is filled which results in a fractional loss of $2(1-\cos\alpha_o)$ of the Ar^+ flux, that is the fraction of the 4π steradians in velocity space occupied by the loss cone. If $p<1$, then we simply use τ_b in the numerator of (12), for then τ_b is the limiting time for loss-cone emptying. The characteristic times τ_{PI}/p range from minutes at L=1.1 to hours at L=4.0 and so when $p\sim1$, τ_{PI} will be the limiting lifetime in the plasmasphere when compared to τ_{CE} and τ_{ECS}. However due to the tendency to approach the limiting flux condition, it is likely that $p>>1$, except for a relatively short period immediately after beam deposition of the Ar^+. Thus the loss of Ar^+ by pitch angle scattering induced by plasma wave turbulence generated by these ions is negligible compared to the other two loss mechanisms discussed earlier. We note that the turbulence may nonetheless be high enough to significantly affect other plasmasphere plasma components.

Possible Environmental Impact: Communications

From our discussion of beam propagation through the plasmasphere and the resulting deposition of energetic Ar^+ in substantial quantities over distances of several earth radii and with lifetimes of up to a year, we see that substantial changes may be expected in the near earth plasma environment. In this section we deal specifically with the effects on terrestrial communications of the enhanced precipitation of energetic ions induced by the 5 keV Ar^+ beam. It is well known that enhanced precipitation of energetic particles occurring during solar flares can seriously disrupt these links (Argo and Hill, 1978; Wong et al, 1978; Prettie, 1978). Fortunately, these naturally occurring disruptions are of relatively short duration ($\sim$ days). However, in the scenario which we present here, there is the potential for communications disruptions over periods of decades as a consequence of the continuous construction of an SPS fleet.

Due to their initial injection almost perpendicular to the local ambient magnetic field the deposited energetic Ar^+ possess a high level of pitch angle anisotropy. This pitch angle anisotropy as discussed in the earlier sections provides the free energy which drives plasma instabilities and hence plasma turbulence. In addition to the plasma turbulence driven by the energetic Ar^+ deposited by the beam, short duration turbulence is also generated by the beam itself as it propagates outward through the plasmasphere. Instabilities expected in this case include the beam-plasma instability driven by the beam's high velocity, drift wave instabilities driven by the density gradient of Ar^+ at the beam's

surface, and the Kelvin-Helmholtz instability driven by the velocity gradient near the beam's surface resulting from the nonuniformity of the polarization electric field. Due to the beam's short residence time (100-200 sec) in the plasmasphere the effects of these plasma instabilities on the beam's attenuation will most likely be minor as discussed earlier. The plasma turbulence will tend to both isotropize Ar^+ as well as the various naturally occurring components of the plasmasphere population. In particular the radiation belt ions will be affected. These ions, mostly protons, are characterized by high energies and fluxes. For energies E>50.MeV, fluxes greater than $10^4 cm^{-2}$ are encountered between L=1.2 and L=1.8 and when E>1.0 MeV fluxes above 10^5 cm^{-2} exist beyond L=2.0 (Hess, 1968). The high fluxes of high energy protons exist precisely in the region of $L \lesssim 2.0$ where most of the Ar^+ deposition occurs as shown in Figure 4. Since the turbulence level will be proportional to the number density of Ar^+, precipitation effects may be substantial in the inner radiation belt. The precipitating protons will have energies up to ~100 MeV and hence may be expected to have effects similar to those of solar flares. In Figure 6 we show a map of the western hemisphere with the near surface L values projected from the earth's equatorial plane (Stassinopolous, 1970). Since precipitation is expected between L=1.1(LEO) and $L \lesssim 4.5$ (plasmapause), most of effects will occur over a latitude range which is roughly centered about the continental U.S. In Figures 7a and 7b we show the spatial distribution of energetic radiation belt protons for E>50 MeV and E>1.0 MeV. We may estimate the lifetime of the radiation belt protons in the plasma

turbulence generated by the Ar^+ using equation (12). Noting that the bounce times are 0.5 to 1 sec for the MeV energy protons and taking the number of bounce periods required to isotropize the MeV ions as about the same as that of the Ar^+, depletion of radiation belt protons can occur up to two orders of magnitude faster than the Ar^+. We may then expect substantial fluxes of radiation belt protons to precipitate before the Ar^+ turbulence subsides due to the Ar^+ population's approach to a limiting flux condition. As the Ar^+ beam propagates outward during the OTV's trip to GEO a continuous source of anisotropic Ar^+ will exist extending from the OTV's orbit to the plasmapause. Thus precipitation effects will extend over the lifetime of the SPS construction ($\sim$6 mos/station). In addition to the proton precipitation, Ar^+ precipitation due to plasma turbulence may be expected as well as the ionization effects due to precipitating $\sim$5 keV argon neutral atoms resulting from charge exchange. Also direct precipitation will occur at orbits near LEO due to the ion beam velocity spread. The penetration depth of these energetic ions will range from stratospheric altitudes for the more energetic radiation belt protons to mesospheric-thermospheric altitudes for the energetic Ar^+ and Ar (Maeda and Singer, 1961). We note that even if only .01% of the beam energy is converted to plasma turbulence (Palmadesso et al, 1976) the expected wide band wave amplitude characterizing this turbulence will be $\sim 10^5$ mγ which is much greater than the natural wave amplitudes observed closely confined to the earth's magnetic equatorial plane of $\sim$20 mγ (Gurnett, 1976). Thus a 3 order of magnitude enhancement of plasma wave turbulence above its natural maximum level

may be possible. This is consistent with our conclusion that greatly increased ion precipitation may be expected. This expectation is also in agreement with the recent results of the Cameo experiments that involved the release of large quantities of Ba into the magnetosphere (private communication, J. P. Heppner) which may have triggered auroral-type particle precipitation. These experiments are known to have produced much greater than normal r-f scintillations and signal attenuation as determined from monitoring a GEOS-3 pass. This scintillation and attenuation is precisely the type of communication impairment expected from the Ar^+ induced precipitation. Ionospheric scintillation will be produced by ionospheric electron density inhomogenities due to the spatial variation in the precipitating fluxes. The results of these processes will be similar to the conditions experienced during solar flare events with bandspreading and signal fadeout (Wong et al., 1978) occurring.

Summary and Conclusions

In the preceding sections we have described the possible consequences of one aspect of the construction of a large fleet of Solar Power Stations. The part of the construction process considered was the transport of large quantities of materials with total masses in the range of hundreds of thousands of metric tons from low earth orbit to geosynchronous orbit. This orbital transfer procedure would entail the release of millions of kilograms of 5 keV argon ions modifying the near earth plasma environment and producing potentially serious effects on terrestrial communications. The Ar^+ deposited in lifting an SPS to GEO will have a greater total energy content than the ionosphere-plasmasphere system. However if these SPS craft were to be built out of lunar materials as envisioned by some authors (O'Leary, 1978) these consequences could be largely avoided since the energy required to transport materials from the lunar surface to GEO is much less than hauling materials from LEO to GEO. Thus, not only would less propellant be needed but it would be deposited much farther from regions where it may have a direct effect on human terrestrial activity. We conclude, on the basis of our preliminary study, that if a fleet of SPS's were to be fabricated, the use of lunar rather than terrestrial materials would appear to minimize the environmental impacts in addition to economic benefits derived from transportation cost reduction. Terrestrial materials would seem to be a viable alternative in the construction of a less than full scale SPS demonstration facility.

REFERENCES

Argo, P. E. and Hill, J. R. Radio propagation and solar cycle 21, in: Proceedings of the 1978 Symposium on the Effect of the Ionosphere on Space and Terrestrial Systems, Naval Research Lab, (1978).

Crow, J. T., A. T. Forrester and D. M. Goebel, Ion beam propagation across magnetic fields, in: Low-energy Ion Beams 1977, (Eds. K. G. Stephens and J. L. Moruzzi) American Institute of Physics, New York, Pg. 228 (1978).

Davidson, R. C., Methods in Nonlinear Plasma Theory, Academic Press, New York (1972).

Falthammar, C.,-G., Motion of charged particles in the magnetosphere, in: Cosmical Geophysics, (ed. A. Egeland, O. Halter and A. Omholt) Scandinavian University Books (1973).

Glaser, P. E., Solar power from satellites, Physics Today, 30, 30 (Feb. 1977).

Gurnett, D. A., Plasma wave interactions with energetic ions near the magnetic equator, J. Geophys. Res., 81, 2765 (1976).

Hanely, G. and Guttman, C. H., Satellite Power Systems Concept Definition Study: Final Report Executive Summary, Rockwell International, Vol. I, (April 1978a).

Hanely, G. and Guttman, C. H., Satellite Power Systems Concept Definition Study: Final Report Transportation and Operations Analysis, Vol. V, (April 1978b).

Hartle, R. E., Model for rotating and nonuniform planetary exospheres, Phys. Fluids, 14, 2592 (1971).

Heikkila, W. J., Plasma transport through the magnetopause, submitted to Geophys. Res. Lett., (1978).

Hess, W. N., The earth's radiation belt, in: Introduction to Space Science (Eds., W. N. Hess and G. D. Mead), Gordon and Breach, New York, pp. 179-216 (1968).

Hultquist, B., Auroras and Polar Substorms: Observations and Theory, Rev. Geophys., 7, 129 (1969).

Kennel, C. F. and Petschek, H. E., Limit on stably trapped particle fluxes, J. Geophys. Res., 71, 1, (1966).

Maeda, K. and S. F. Singer, Energy dissipation of spiraling particles in the polar atmosphere, Arkiv for Geofysik, Band 3 nr 21, (1961).

Mapleton, R. A., Theory of Charge Exchange, John Wiley and Sons, Inc., (1972).

Mikhailovskii, A. B., Theory of Plasma Instabilities, Vol. 1, Consultants Bureau (1974).

Mikhailovskii, A. B., Electromagnetic instabilities in a non-Maxwellian plasma, In: Reviews of Plasma Physics, Vol. 6 (M. A. Leontovich, ed.) Consultants Bureau (1975).

Montgomery, D. C. and Tidman, D. A., Plasma Kinetic Theory, McGraw-Hill Book Co., New York (1964).

O'Leary, B., Mining the moon and asteroids and living in space, Astronautics and Aeronautics, 16, 20 (March, 1978).

Palmadesso, P., T. P. Coffey, S. L. Ossakow, and K. Papadopoulos, Generation of terrestrial kilometric radiation by a beam driven electromagnetic instability, J. Geophys. Res., 81, 1762 (1976).

Prettie, C. W., Upper limit to the bandspreading and fade rates produced by ionospheric/magnetospheric scintillations, Proc. of the IES, Naval Research Lab. (1978).

Revelle, R. R., Studies in Geophysics: Energy and Climate, National Academy of Sciences, Washington, D.C. (1977).

Schmidt, G., Physics of High Temperature Plasmas, Academic Press, New York (1966).

Schulz, M. and L. J. Lanzerotti, Particle Diffusion in the Radiation Belts, Spring-Verlag, New York (1974).

Spitzer, L., Physics of Fully Ionized Gases, John Wiley and Sons, Inc., (1967).

Stassinopoulos, E. G., World Maps of Constant B, L, and Flux Contours, NASA SP-3054 (1970).

Stedeford, J.B.H. and J. B. Hasted, Further investigations of charge exchange and electron detachment, Proc. Roy. Soc., A227, 466 (1955).

Stuhlinger, E., Ion Propulsion for Space Flight, McGraw-Hill, Inc., New York (1964).

Wong, Y.K., K. C. Yeh and C. H. Liu, Mean arrival time and mean pulse width of signals propagating through an inhomogeneous ionosphere with random irregularities, in: Proceedings of the 1978 Symposium on the Effect of the Ionosphere on Space and Terrestrial Systems, Naval Research Lab. (1978).

Figure Captions

Figure 1. Diagram of LEO to GEO orbital transfer.

Figure 2. Ion beam density n_b and stopping density, n_c as a function of equatorial radial distance L for injection of L_o=1.5 earth radii.

Figure 3. Fraction of ion beam deposited by a given equatorial radial distance, L, for a number of orbital injection points L_o.

Figure 4. Total radial density profile of Ar^+ resulting from a fleet of 10 OTV's transporting materials for one SPS from LEO to GEO.

Figure 5. Ar^+ lifetimes due to charge exchange and electron coulomb scattering, for selected electron energies, as a function of equatorial radial distance, L.

Figure 6. Values of L mapped from the earth's equatorial plane to a 100 km altitude (after Stassinopolous, 1970).

Figure 7. Radiation belt proton fluxes for energies (a) E > 50 MeV (b) E>1.0 MeV (after NASA SP-8116, 1975).

Table 1. Orbital Transfer Vehicle (OTV) beam plasma parameters.

TABLE 1.

PLASMA PARAMETERS/OTV (Orbital Transfer Vehicle)

Single Thruster:

Thrust = 14.5 N

Ar^+ release Rate = 1.4×10^{21} ions/s

259 Thrusters (Area $\sim 10^3 m^2$):

Number Flux = $3.4 \times 10^{16}/cm^2$-s

3×10^{30} Ar^+ ions Released on Upleg

Peak Ar^+ Density $\sim 3 \times 10^9/cm^3$

Averaged Over Magnetosphere:

30 Ar^+ ions/cm^3 (Ambient Density Ranges from 10^4 to <10 ions/cm^3

150 Kev/cm^3 (Ring Current $\sim$ Few Mev/cm^3)

Note: As Many as 10 OTV's May be Required for 1 SPS

ORBITAL TRANSFER VEHICLE (OTV) 1.5×10^6 kg

PAYLOAD 4×10^6 kg

Ar PROPELLANT

UP 2×10^5 kg

DOWN 6×10^4 kg

EACH SOLAR POWER SATELLITE (SPS) REQUIRES ~10 TRIPS

2 SPS/YEAR INITIALLY

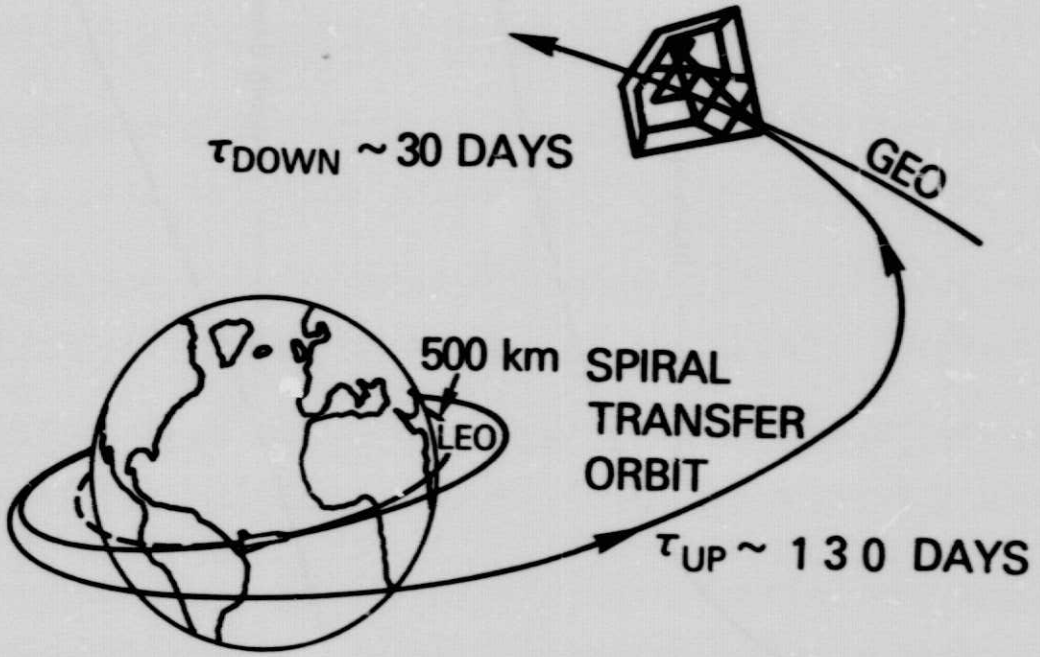

POWER (P) LEVEL OF ION PROPULSION SYSTEM ~300 MW

FLIGHT TIME τ = E/P WHERE E IS ENERGY NEEDED TO CONVERT PROPULSION MASS TO 5 KEV Ar^+ IONS.

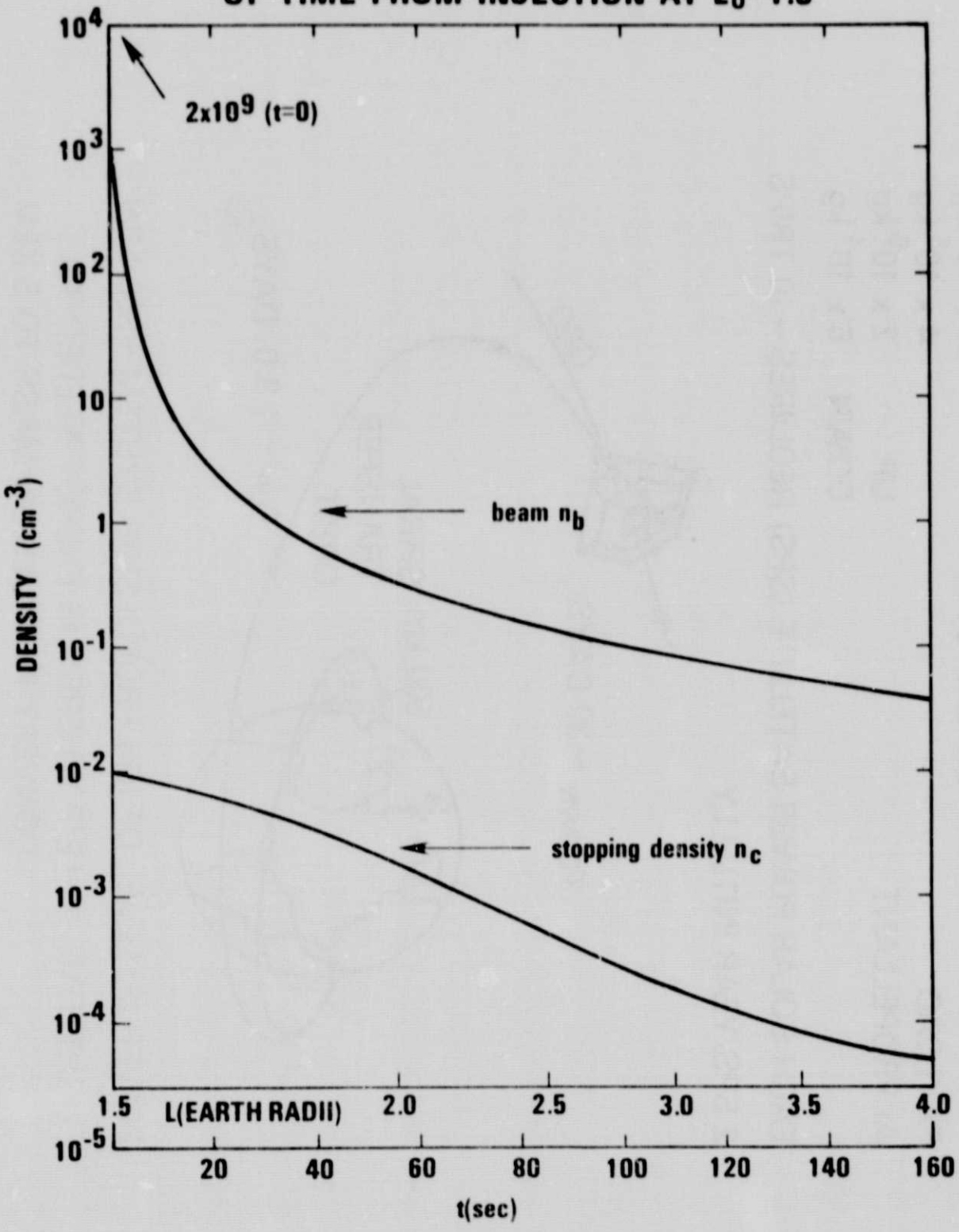
BEAM DENSITY DECREASE AS A FUNCTION OF TIME FROM INJECTION AT L_0=1.5
10^4
10^3
10^2
10
1
10^{-1}
10^{-2}
10^{-3}
10^{-4}
10^{-5}
DENSITY (cm^{-3})
$2x10^9$ (t=0)
beam n_b
stopping density n_c
1.5
L(EARTH RADII)
2.0
2.5
3.0
3.5
4.0
20
40
60
80
100
120
140
160
t(sec)

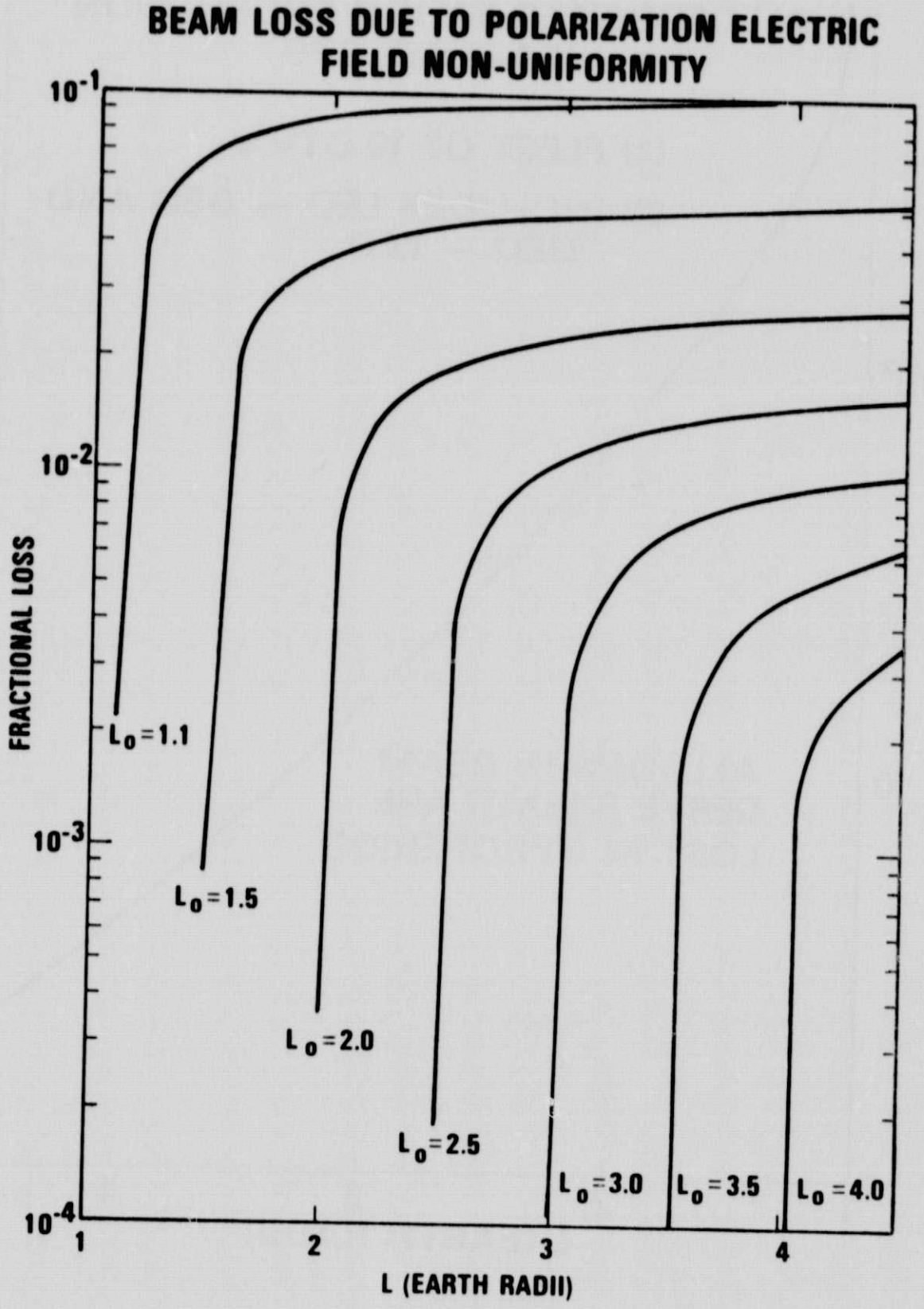
BEAM LOSS DUE TO POLARIZATION ELECTRIC FIELD NON-UNIFORMITY
FRACTIONAL LOSS
10-1
10-2
10-3
10-4
1
2
3
4
L (EARTH RADII)
L0=1.1
L0=1.5
L0=2.0
L0=2.5
L0=3.0
L0=3.5
L0=4.0

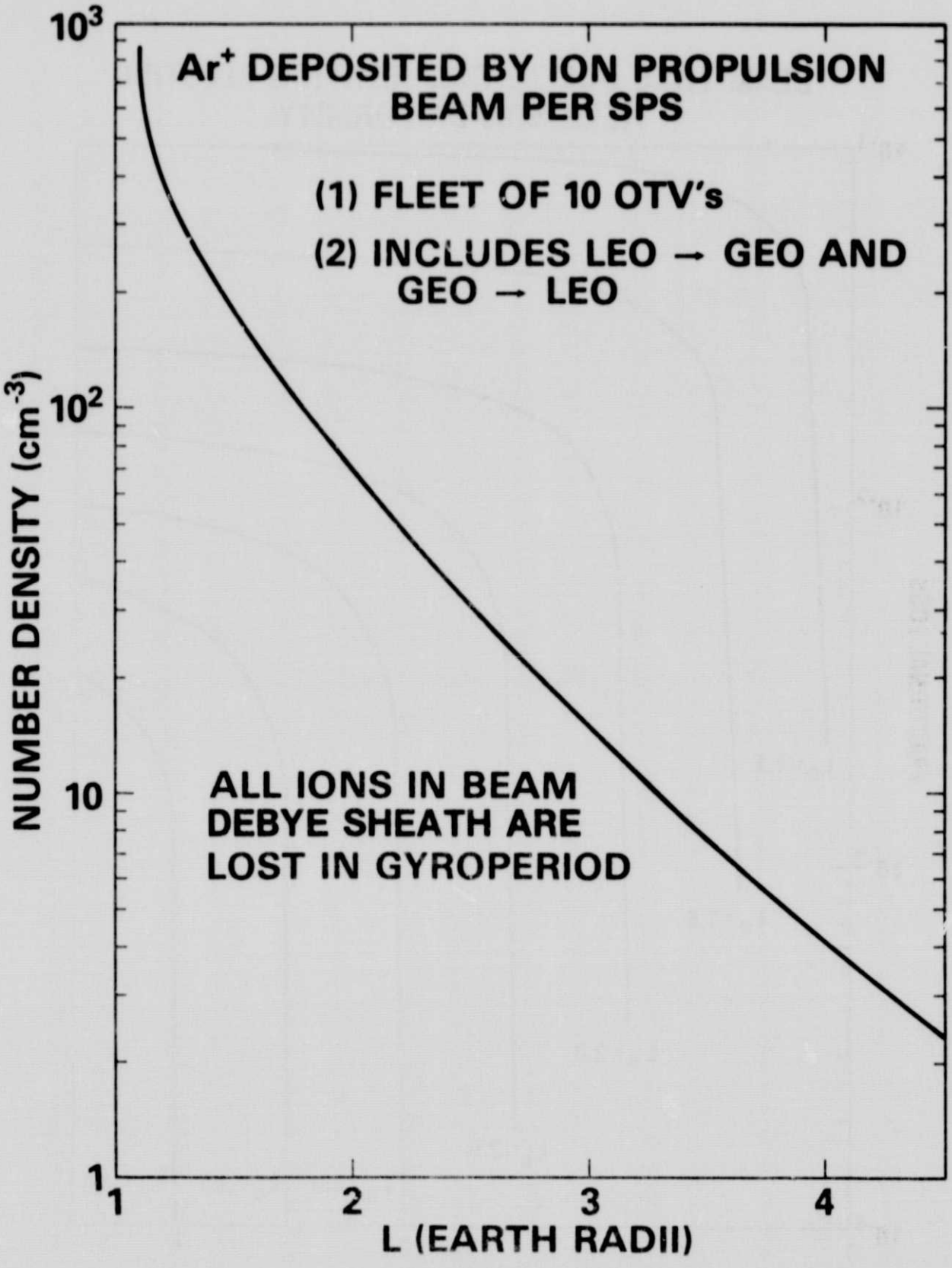
Ar^+ DEPOSITED BY ION PROPULSION BEAM PER SPS
(1) FLEET OF 10 OTV's
(2) INCLUDES LEO → GEO AND GEO → LEO
ALL IONS IN BEAM DEBYE SHEATH ARE LOST IN GYROPERIOD
NUMBER DENSITY (cm^{-3})
10^3
10^2
10
1
1
2
3
4
L (EARTH RADII)

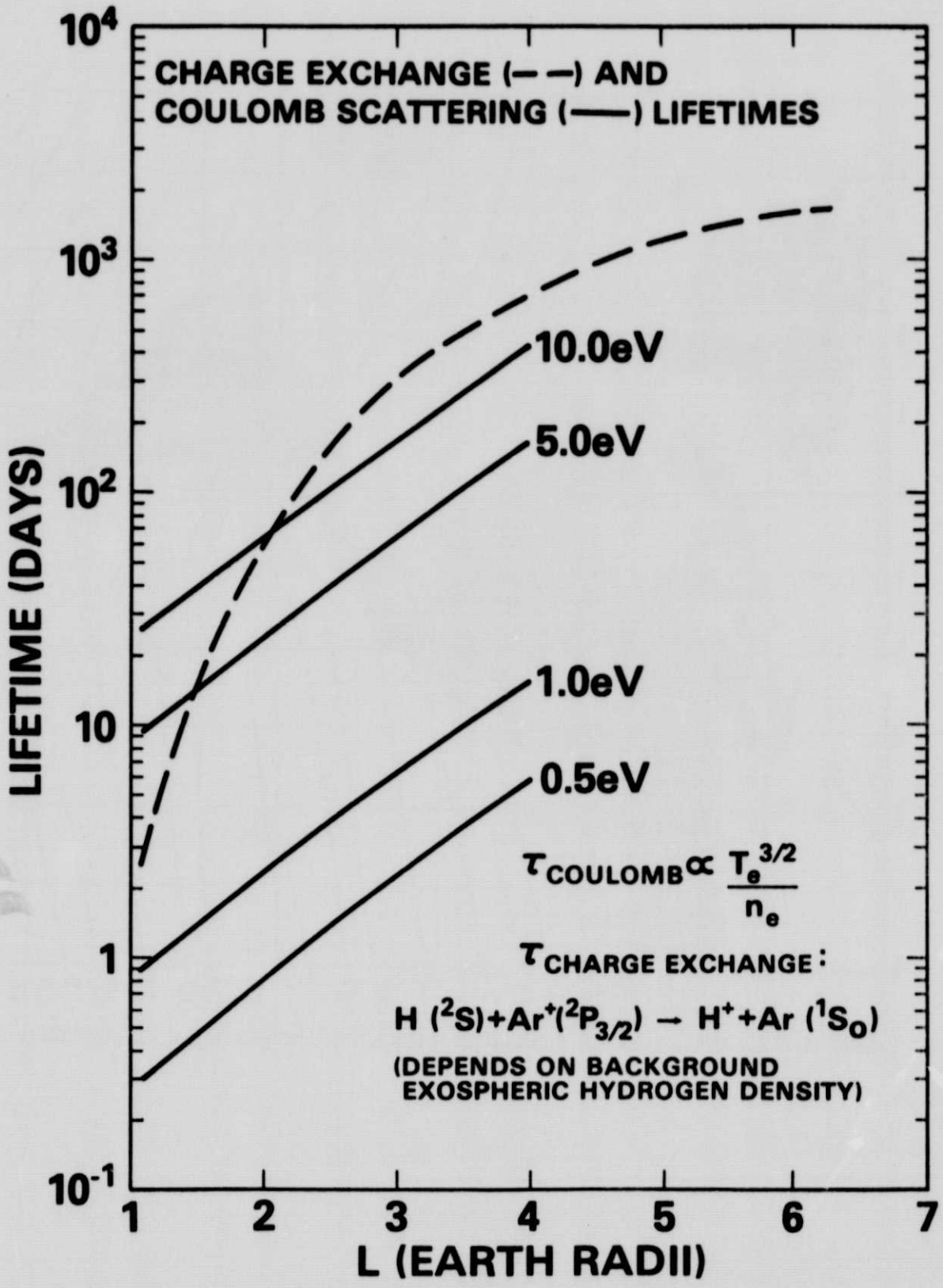
CHARGE EXCHANGE (— —) AND
COULOMB SCATTERING (——) LIFETIMES
LIFETIME (DAYS)
L (EARTH RADII)
10.0eV
5.0eV
1.0eV
0.5eV
$\tau_{COULOMB} \propto \frac{T_e^{3/2}}{n_e}$
$\tau_{CHARGE\ EXCHANGE}$:
$H\ (^2S) + Ar^+(^2P_{3/2}) \rightarrow H^+ + Ar\ (^1S_o)$
(DEPENDS ON BACKGROUND
EXOSPHERIC HYDROGEN DENSITY)

LINES OF CONSTANT L (EARTH RADII)

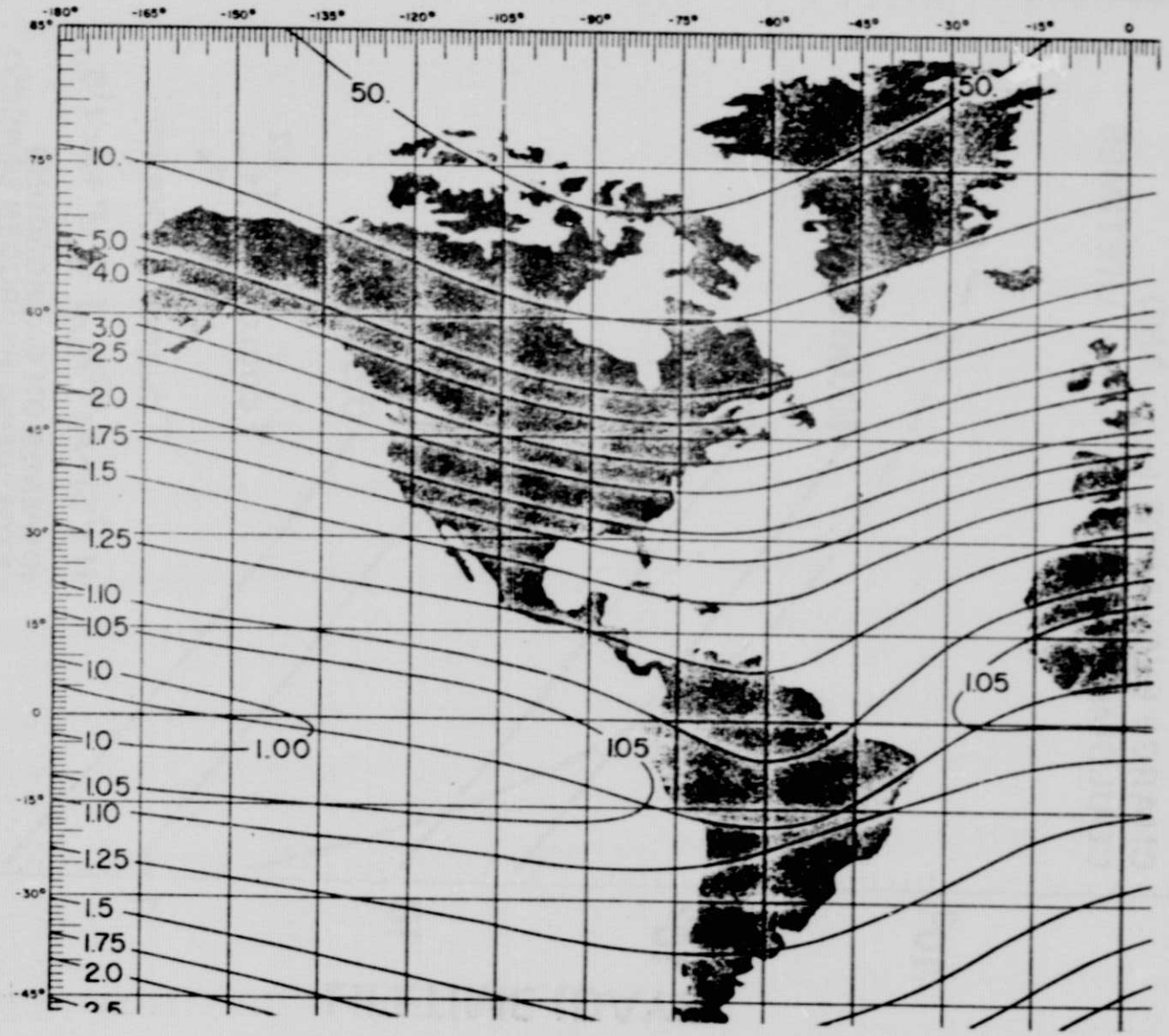

a

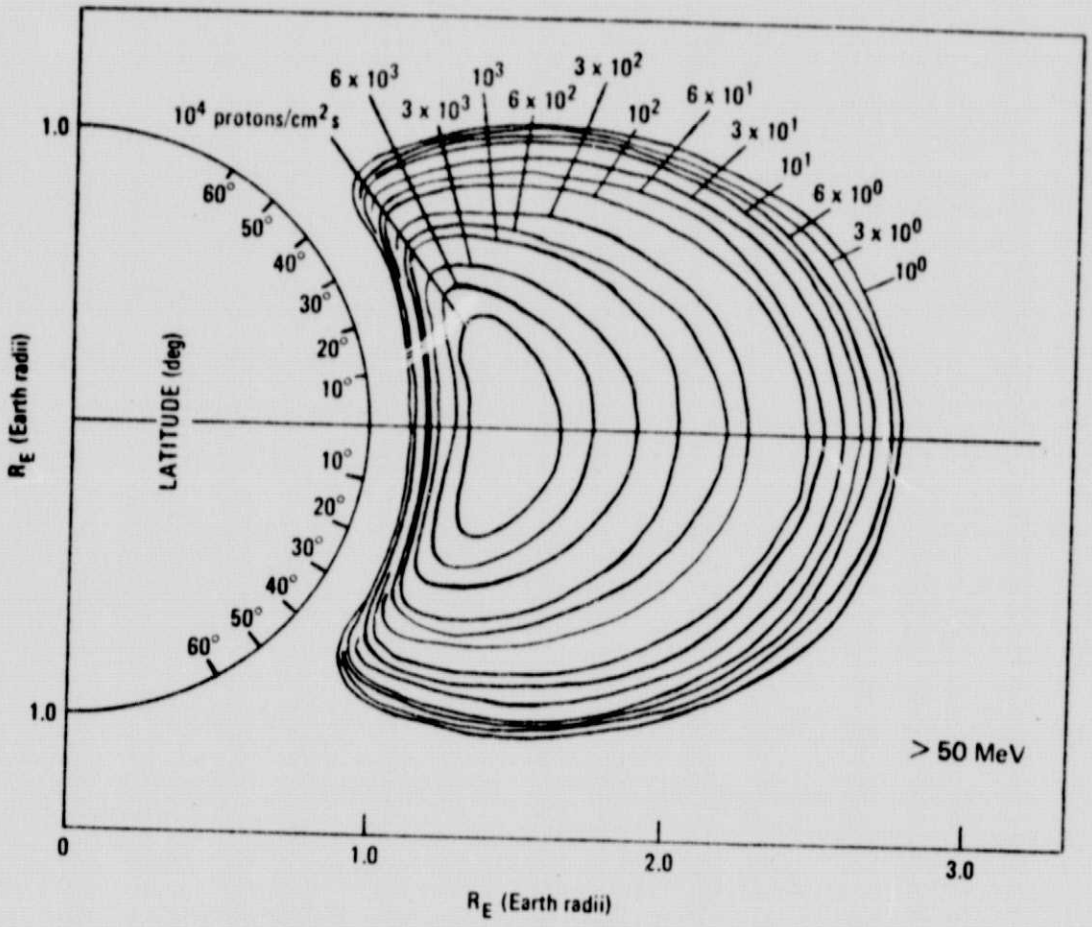
10^4 protons/cm^{2}s
6 x 10^3
3 x 10^3
10^3
6 x 10^2
3 x 10^2
10^2
6 x 10^1
3 x 10^1
10^1
6 x 10^0
3 x 10^0
10^0
1.0
60°
50°
40°
30°
20°
10°
LATITUDE (deg)
R_E (Earth radii)
> 50 MeV
0
1.0
2.0
3.0
R_E (Earth radii)

b

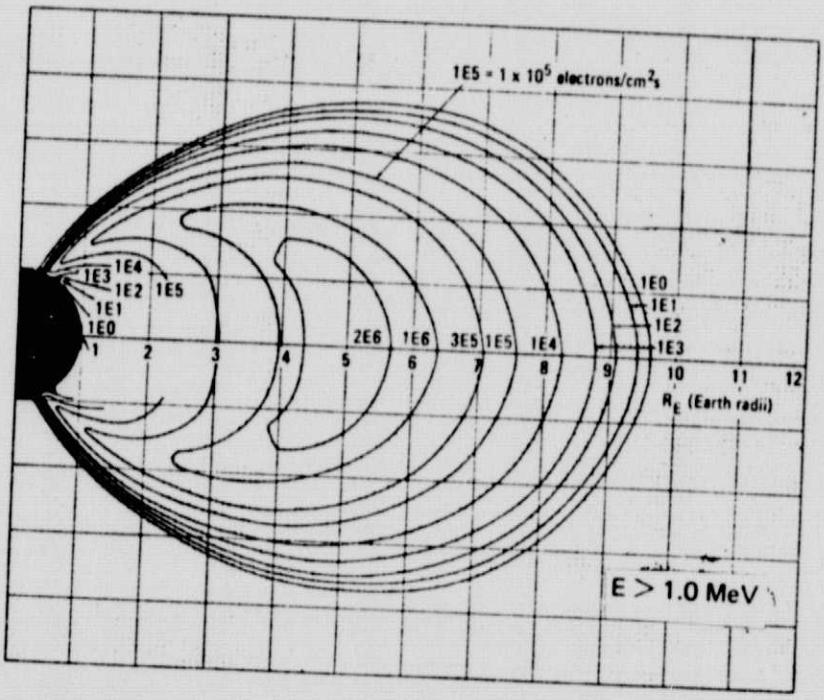
1E5 = 1 x 10^5 electrons/cm^{2}s
1E3
1E4
1E2
1E5
1E1
1E0
1
2
3
4
5
2E6
1E6
6
3E5
7
1E5
1E4
8
9
1E0
1E1
1E2
1E3
10
11
12
R_E (Earth radii)
E > 1.0 MeV